Research article

Journal of Applied Toxicology

Received: 18 November 2015, Revised: 28 December 2015, Accepted: 13 January 2016 Published online in Wiley Online Library: 3 March 2016

(wileyonlinelibrary.com) DOI 10.1002/jat.3304

Optimization of an air–liquid interface exposure system for assessing toxicity of airborne nanoparticles

Siiri Latvala[a], Jonas Hedberg[b], Lennart Möller[c], Inger Odnevall Wallinder[b], Hanna L. Karlsson[d] and Karine Elihn[a]*

Abstract: The use of refined toxicological methods is currently needed for characterizing the risks of airborne nanoparticles (NPs) to human health. To mimic pulmonary exposure, we have developed an air–liquid interface (ALI) exposure system for direct deposition of airborne NPs on to lung cell cultures. Compared to traditional submerged systems, this allows more realistic exposure conditions for characterizing toxicological effects induced by airborne NPs. The purpose of this study was to investigate how the deposition of silver NPs (AgNPs) is affected by different conditions of the ALI system. Additionally, the viability and metabolic activity of A549 cells was studied following AgNP exposure. Particle deposition increased markedly with increasing aerosol flow rate and electrostatic field strength. The highest amount of deposited particles (2.2 μg cm^{-2}) at cell-free conditions following 2 h exposure was observed for the highest flow rate (390 ml min^{-1}) and the strongest electrostatic field (±2 kV). This was estimated corresponding to deposition efficiency of 94%. Cell viability was not affected after 2 h exposure to clean air in the ALI system. Cells exposed to AgNPs (0.45 and 0.74 μg cm^{-2}) showed significantly ($P < 0.05$) reduced metabolic activities (64 and 46%, respectively). Our study shows that the ALI exposure system can be used for generating conditions that were more realistic for *in vitro* exposures, which enables improved mechanistic and toxicological studies of NPs in contact with human lung cells.

Keywords: ALI; nanotoxicology; in vitro; silver; nanoparticles; electrostatic; A549

Introduction

Inhalation is an important exposure route for airborne nanoparticles (NPs; < 100 nm) in humans (ICRP, 1994). Workers in the nanomaterial industry are a likely group to become exposed to manufactured NPs in their pristine form (Schäfer *et al.*, 2013). Furthermore, occupational settings in the industry constitute conditions in which unintentionally produced metal-containing NPs are known to exist (Bergamaschi, 2009). Considering the expanding development and use of nanomaterials in various fields, rapid screening of their possible hazards is essential for ensuring the safety of workers, consumers and the environment. The importance of characterizing risks of nanomaterials has been strongly acknowledged in society, and methods and approaches applying the principle of the three Rs (replacement, reduction and refinement of *in vivo* animal testing) are prioritized (ECHA, 2015; Russell *et al.*, 1959). As the nanomaterial industry is expanding, there is a growing need for reliable, yet rapid, methods to screen potential health hazards of NPs. Structure–activity relationships are examples of potential tools for screening large numbers of materials for hazards in relation to their inherent properties. However, the development of these screening tools is dependent on the availability of relevant toxicological and physicochemical (or structural) data of a set of materials on which these models are based. Validated *in vitro* methods are thus considered necessary for supporting the construction of such models for nanomaterials (Schäfer *et al.*, 2013).

The human lung has a large surface area as well as a high sensitivity and permeability for small-sized particles. Thus, it is a very likely site where airborne NPs may induce adverse effects. However, there are limitations to many of the currently used toxicological tests for NPs concerning pulmonary exposure. Despite the physiological characteristics of the human lung, most *in vitro* studies of NP toxicity have been conducted using submerged cell cultures. The limitations of applying these conventional *in vitro* methods for airborne NPs have been widely acknowledged (Paur *et al.*, 2011; Wittmaack, 2011a, 2011b). Thus, there is an expressed need for refined approaches (Grass *et al.*, 2010). It is not only challenging to define

*Correspondence to: Karine Elihn, Department of Environmental Science and Analytical Chemistry, Atmospheric Science Unit, Stockholm University, SE-106 91 Stockholm, Sweden
E-mail: karine.elihn@aces.su.se

[a]Department of Environmental Science and Analytical Chemistry, Atmospheric Science Unit, Stockholm University, SE-106 91 Stockholm, Sweden

[b]Division of Surface and Corrosion Science, School of Chemical Science and Engineering, KTH Royal Institute of Technology, SE-100 44 Stockholm, Sweden

[c]Department of Biosciences and Nutrition, Unit for Analytical Toxicology, Karolinska Institute, SE-141 83 Huddinge, Sweden

[d]Division of Biochemical Toxicology, Karolinska Institute, Institute of Environmental Medicine, SE-171 77 Stockholm, Sweden

Journal of Applied Toxicology

the effective dose of particles in submerged cell culture systems, but also some of the particle properties, such as their size, surface charge, solubility, transformation or agglomeration state, can be affected and change with time due to the chemical properties and composition of the cell culture medium (Cronholm *et al.*, 2011; Limbach *et al.*, 2005; Teeguarden *et al.*, 2007). These properties have all been shown to be important for the fate and effect of NPs. Furthermore, adsorption of biomolecules, such as proteins and lipids, in solution and on the surface of NPs, influences their stability and transformation in biological environments and hence, influences their fate (Cronholm *et al.*, 2011; Karlsson *et al.*, 2013; Lundqvist *et al.*, 2008). These processes and mechanisms may be very different if the particles are present in an aerosol or if they are immersed in a liquid.

Several advanced *in vitro* approaches have been described for the exposure of human lung cells to airborne NPs (Kim *et al.*, 2013; Lenz *et al.*, 2009; Savi *et al.*, 2008). These approaches are based on air–liquid interface (ALI) methods, where cells are cultured on thin porous membranes in cell culture inserts with cell culture medium only on the basal side of the insert. The aim of these methods is to provide an *in vitro* exposure setting that is more representative of pulmonary exposure. Compared to submerged exposure systems, ALI methods for example permit the particles to maintain their intrinsic characteristics until they reach the cells, thereby allowing for a better control of the effective dose (Paur *et al.*, 2011). However, because the motion and deposition of NPs are largely controlled by diffusion (Hinds, 1999), efficient deposition can be difficult to achieve *in vitro*. Therefore, particle deposition is in some ALI exposure systems enhanced by applying an electrostatic field that enables the attraction of charged particles towards an electrode of the opposite charge (Savi *et al.*, 2008).

Silver is among the most commonly used metals in NPs (Behra *et al.*, 2013). Owing to its bactericidal properties, silver NPs (AgNPs) are currently used in several medical applications (Tarimala *et al.*, 2006), but also in textiles, cosmetics and electronics (Behra *et al.*, 2013). As in the case of many other engineered NPs, occupational exposure is the primary concern for human health effects induced by AgNPs (Behra *et al.*, 2013). Owing to the frequent use of AgNPs and the large span of the already published data on their potential adverse health effects, AgNPs were chosen as model particles in this study.

The aims of this study were to develop and analyze the performance of a new aerosol exposure system for *in vitro* toxicological and mechanistic studies of metal-containing airborne NPs in contact with human lung cells. This was achieved by determining the effects of different exposure parameters, such as strength of the applied electrostatic field and aerosol flow rate, on the deposition efficiency of AgNPs, but also on the viability and metabolic activity of human lung cells. As a large fraction of the inhaled NPs are likely to deposit in the alveolar region of the human lung, a human type II alveolar epithelial cell line (A549) was chosen for this study (Oberdörster *et al.*, 2005). This cell line has previously been used in studies of NP toxicity and in studies using ALI exposure methods (Foldbjerg *et al.*, 2011; Karlsson *et al.*, 2008, 2009; Lenz *et al.*, 2009). In addition to describing the performance of the exposure system, this study demonstrates that even low amounts of deposited AgNPs in ALI can induce acute effects on the metabolic activity of A549 cells.

Materials and methods

Particle generation

Airborne AgNPs were generated from bulk Ag (Goodfellow Cambridge Ltd., Huntingdon, England; 99.997% purity) through nucleation in a high-temperature furnace as described by Elihn *et al.* (2013). To create a vapor pressure of 133 Pa (1 Torr), the temperature was set to 1200 °C. The generated aerosol was transported in stainless steel tubes using a flow of nitrogen gas (99.996 vol% N_2, 1500 ml min^{-1}) to either the ALI exposure system, or a differential mobility particle sizer (DMPS) for on-line particle size distribution measurements.

The aerosol passed through a bipolar charger to reach an equilibrium charge distribution before the DMPS or the ALI exposure system. The aerosol was adjusted to physiological conditions (20 vol% O_2 and 5 vol% CO_2) and humidified (20% relative humidity, 37 °C) with a gas humidifier (MH-110-12S-4; Perma Pure LLC, Lakewood, NJ, USA) filled with MilliQ-water (18.2 MΩcm) before reaching the exposure chambers (Fig. 1). Owing to practical reasons, the humidity was measured (Humidity and Temperature Transmitter, HMT333; Vaisala Oyj, Helsinki, Finland) before the aerosol reached the cell exposure chambers. Therefore, the exact humidity in the cell exposure chambers is not known. However, due to evaporation of water from the cell culture media, the relative humidity of the aerosol in contact with the cells is most likely higher than 20%.

On-line particle characterization

Particle size distributions were monitored with a DMPS before each experiment. A DMPS consists of a differential mobility analyzer, which measures the electrical mobility diameter of the particles with the detection interval of 10–800 nm, and of a condensation particle counter (model 3022; TSI GmbH, Aachen, Germany), as described previously by Elihn *et al.* (2013). A DMPS was also used as a rapid method for determining how the particle deposition efficiency was affected by changes in exposure conditions, such as the strength of the applied electrostatic field or the aerosol flow rate. For monitoring these changes, the DMPS was connected downstream of the ALI system.

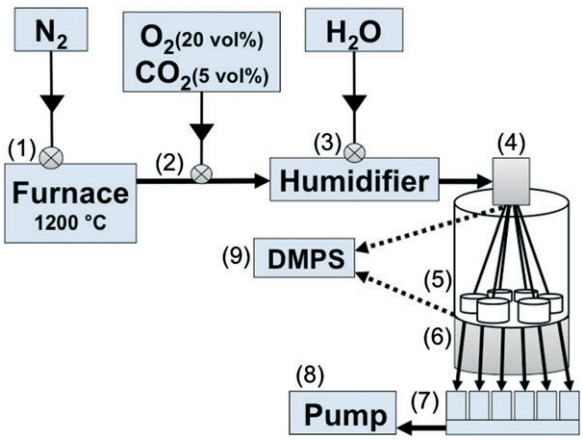

Figure 1. Schematic illustration of the electrostatic air–liquid interface exposure system. (1) Silver nanoparticles are generated in a high temperature furnace (1200 °C). (2) Particles are transported further in N_2, into which a mixture of O_2 and CO_2 is added. (3) Aerosol is humidified, and (4) particles are charged with a bipolar charger. (5) Aerosol is directed into six separate exposure chambers, two of which are equipped with filters. (6) Particle deposition is enhanced by applying an electrostatic force between the aerosol inlet and an electrode underneath the exposure chambers. (7) Critical orifices control the aerosol flow rate individually for each exposure chamber. (8) Aerosol is driven through the system by a pump. (9) Alternatively, the aerosol is directed to a DMPS for on-line particle characterization either before or after the exposure chambers. DMPS, differential mobility particle sizer.

Particle deposition in the air–liquid interface system

After measuring the particle size distribution, the aerosol flow was directed into the exposure chambers of the ALI exposure system. The temperature of the humidified aerosol was approximately 37 °C before entering the exposure chambers. Cell culture inserts containing A549 cells, or inserts without cells, were positioned in the exposure chambers directly before exposure initiation. Three to six inserts (depending on the aerosol flow rate) were exposed in the chambers simultaneously for 2 h. Separate critical orifices were used for controlling the aerosol flow (100, 214 or 390 ml min^{-1} per insert of 4.2 cm^2) through each of the six exposure chambers (Fig. 1). A schematic illustration shows the dimensions of the aerosol inlet and how the aerosol flow is directed to the cells in each exposure chamber (Fig. 2). To enhance the deposition of NPs, an electrostatic field was applied between the aerosol inlet and a metal plate underneath the exposure chambers, acting as electrodes (with a distance of 10.5 mm). The applied field was alternating between a positive and a negative charge (±0.1–4 kV) at a frequency of 0.24 Hz.

Each exposure chamber included one cell culture insert with a total surface area of 4.2 cm^2. To obtain simultaneous negative control treatments (clean air exposure), two separate hydrophobic filters (Headline filters; In-line filter; Grade DIF-LN40) were used to remove all particles from the aerosol entering into two of the exposure chambers. The four remaining chambers received a non-filtered aerosol. After each experiment, the cell culture inserts were either taken to off-line characterization to assess the amount of deposited AgNPs, or to analyze the cell toxicity.

Off-line particle characterization

To quantify the total amount of particle deposition on the insert membranes, the membranes were analyzed gravimetrically after exposing cell-free inserts to AgNPs for 2 h in the ALI system. Different exposure parameters (aerosol flow rates of 100, 214 and 390 ml min^{-1} and applied electrostatic field strengths of ±0.5, ±1 and ±2 kV) were used to investigate their influence on the deposition efficiency of AgNPs. Before exposure, the cell culture insert membranes were cut out and positioned at the bottom of intact cell culture inserts. The mass of each membrane was measured before and after exposure to AgNPs to determine the deposited mass of Ag (MT5, precision: 1 μg; Mettler-Toledo LLC, Columbus, OH, USA). Before weighing, the membranes were conditioned for 24 h in a room with controlled temperature (20 ± 0.5 °C) and relative humidity (50 ± 2%).

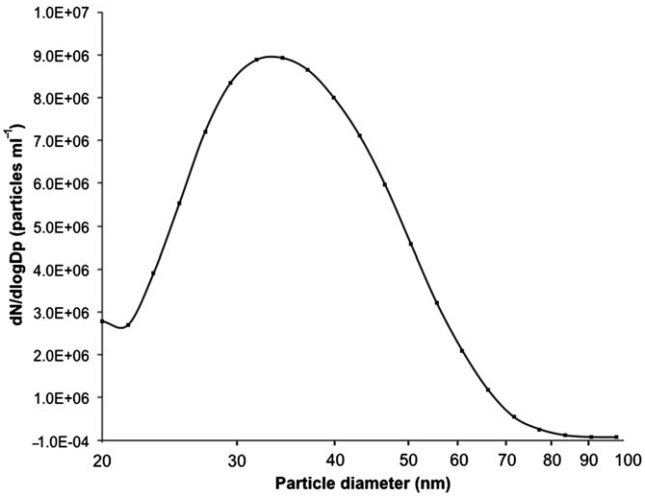

Figure 2. Size distribution of airborne silver nanoparticles (3.1×10^6 particles ml^{-1}, geometric mean diameter: 35 nm, geometric standard deviation: 1.4) generated with a high temperature furnace and measured with a differential mobility particle sizer before entering the air-liquid interface system.

The gravimetric measurements were verified by chemical analyses of a selection of samples using atomic absorption spectroscopy (AAS). The samples were chosen to include the following exposure conditions: an aerosol flow rate of 100 ml min^{-1} with an applied electrostatic field strength of ±1 or ±2 kV, and a flow rate of 390 ml min^{-1} with a field strength of ±1 or ±2 kV. Triplicate samples were analyzed for each condition. Each exposed membrane was positioned into an acid-cleaned plastic tube (10 vol% HNO_3 for 24 h, rinsed well with MilliQ-water) along with 6 ml of 32.5 vol% HNO_3 (Suprapur; Sigma-Aldrich Co. LLC, St. Louis, MO, USA). The samples were sonicated (10 min, Transsonic Digital, power-level 9; Elma Schmidbauer GmbH, Singen, Germany) in an ultrasonic water bath. The supernatants were transferred into glass tubes into which 1 ml H_2O_2 (puriss p.a.; Fluka, Sigma-Aldrich Co. LLC, St. Louis, MO, USA) was added. The plastic tubes were further rinsed with 4 ml MilliQ-water, which was added into the glass tubes to ensure complete transfer of Ag possibly remaining in the tube. The samples were digested via ultraviolet treatment (Metrohm 705 ultraviolet digester, 95 °C for 2 h) before total Ag concentrations were quantified with AAS as described previously by Hedberg *et al.* (2014). Briefly, an AAnalyst 800 instrument was used with calibration standards at 0, 7.5, 15, 30 and 45 μg l^{-1} Ag, which were prepared from a standard solution (1 g l^{-1} Ag; PerkinElmer, St., Waltham, MA, USA). The detection limit of the analysis was estimated to 5 μg l^{-1}. Triplicate readings were analyzed for each sample. Control samples of known Ag concentrations were analyzed in parallel, and showed acceptable recoveries (85−100%).

The amount of cellular Ag exposure was determined by exposing A549 cells to AgNPs for 2 h at the same conditions as for the cytotoxicity investigation (aerosol flow rates of 214 and 390 ml min^{-1} with an applied electrostatic field of ±1 kV). Total Ag concentrations were quantified from the cell-containing insert membranes by means of AAS as described for the cell-free membranes, with the exception, that 1.5 ml of 37% HCl (AR grade; Sigma-Aldrich) was added to the samples (5% HCl in the final solutions). This was done to avoid trace-levels of Cl^- ions in the cell cultures causing the formation of insoluble complexes with Ag^+ ions. Parallel measurements of the amount of cellular Ag by means of inductively coupled plasma mass spectrometry revealed similar findings as the AAS approach (data not shown).

In addition to the quantitative measurements, the effects of different conditions on the deposition patterns of AgNPs on the insert membranes were investigated visually. These experiments were conducted at cell-free conditions with aerosol flow rates of 100, 214 and 390 ml min^{-1} and electrostatic field strengths of ±0.5, ±1 and ±2 kV. Based on these analyses, an aerosol flow rate of 214 ml min^{-1} and electrostatic field strength of ±1 kV was chosen for more in-depth analyses of the particle deposition patterns using transmission electron microscopy (TEM). Samples for TEM were prepared by placing carbon-coated copper TEM grids on the cell culture membranes, which were then exposed to the AgNPs. TEM investigations were performed using a Hitachi (Hitachi High Technologies America Inc., Tokyo, Japan) HT7700 microscope operating at 100 kV. TEM images were recorded in bright field mode.

Journal of Applied Toxicology

Cell culture

A549 cells (continuous human type II alveolar epithelial cell line; American Type Culture Collection, ATCC, Manassas, VA, USA) were cultured in Dulbecco's minimal essential medium (DMEM, cat. no. 41965-039; Gibco® Invitrogen™, Thermo Fisher Scientific Inc., Waltham, MA, USA) supplemented with 10% fetal bovine serum (European grade; Biological Industries Israel Beit-Haemek Ltd., Kibbutz Beit-Haemek, Israel), 1 mM sodium pyruvate (Gibco® Life Technologies, Thermo Fisher Scientific Inc., Waltham, MA, USA), 100 units ml^{-1} penicillin and 100 $\mu g\ ml^{-1}$ streptomycin (Pen Strep; Gibco® Life Technologies). DMEM with these supplements is here denoted $DMEM^+$. Cells were cultured in cell culture flasks in 5 vol% CO_2 atmosphere (< 99% relative humidity, 37 °C) and used between passages 6 and 10. Cells were seeded in BD Falcon™, Corning Technologies Pvt Ltd., Maharashtra, India cell culture inserts (cat. no. 353493, with 0.4 μm pore size and pore density of 1.0×10^8 pores cm^{-2}) 24 h before exposure in a density of 0.08×10^6 cells cm^{-2} and grown to confluence.

Before each experiment, cell medium was removed from the apical side and the inserts were transferred to the exposure chambers of the ALI system. Cells were nourished from the basal side of the insert with 3.3 ml $DMEM^+$ HEPES cell culture medium (DMEM; cat. no. 22320-022, Gibco® Invitrogen, supplemented with 10% fetal bovine serum, 1 mM sodium pyruvate, 100 units ml^{-1} penicillin and 100 $\mu g\ ml^{-1}$ streptomycin).

Cell viability

Cells in the ALI system were exposed to airborne AgNPs from the apical side. The cells were kept in the ALI system for 2 h, after which the exposure was terminated or continued in a cell incubator (5 vol% CO_2, < 99% relative humidity, 37 °C). Each experiment was performed in triplicate with three to six inserts including two to four that were exposed to AgNPs and one to two clean air exposure inserts used as negative controls. These latter cells were kept in the ALI system during the AgNP exposures, but were only exposed to an air stream from which all particles were removed by filtration. During each exposure, one to two inserts, with media only on the basal side, were kept in the cell incubator as additional controls.

In addition to the control treatments during the AgNP exposures, additional control experiments were performed to detect possible effects induced by the system itself, the filtration procedure of the aerosol, or by the applied electrostatic field on the cells. Cells were exposed to clean air (no AgNPs) for 2 h in the ALI system at the very same exposure conditions as in the AgNP exposures, except for the lack of an applied electrostatic field.

Cell viability was determined with two methods. Trypan blue hassay was performed as described by Elihn *et al.* (2013), where non-stained cells were considered viable due to their intact membranes. Cell viability was also studied with the Alamar blue assay, which provides an indication of the metabolic activity of the cells. Inserts were transferred into six-well plates, where 1.5 ml of 10% AlamarBlue® (Invitrogen, Life Technologies, Thermo Fisher Scientific Inc., Waltham, MA, USA) solution in $DMEM^+$ was added on both the apical and the basal sides, while keeping the inserts at dark conditions. Cells were incubated for 3 h in 37 °C and 5% CO_2. Solution from the apical side of each insert was transferred in three wells (80 μl per well) on a 96-well plate. Fluorescence was measured in a plate reader (SpectraMax® Gemini EM Microplate Reader; Molecular Devices, CA, USA) using 560 nm excitation and 590 nm emission wavelengths. Dispersions of CuO NPs (20–40 nm; Sigma-Aldrich) at 40 $\mu g\ cm^{-2}$ in $DMEM^+$ were used as a positive control treatment. Negative controls kept in the cell incubator were included in both assays.

Statistical analysis

Statistical analyses were performed in R (version 3.1.1, R Core Team 2014) using a statistical significance level set to 0.05. Data were analyzed with the non-parametric Kruskal–Wallis analysis of variance. The Tukey honest significant difference test was used for *post-hoc* testing.

Results

Silver nanoparticles

The number concentration of freshly generated AgNPs was 3.1×10^6 particles ml^{-1} (Fig. 3). The polydisperse aerosol had a particle geometric mean diameter of 35 nm and a ±geometric standard deviation of 1.4 (Fig. 3). TEM images show particle morphologies as well as sizes of deposited primary particles and agglomerates (Fig. 4).

The total amount of Ag deposited on cell-free insert membranes (measured gravimetrically) after 2 h exposure to AgNPs at three different aerosol flow rates (100, 214 and 390 ml min^{-1}) and at two different applied electrostatic field strengths (±1 and ±2 kV) are given in Table 1 When presented as the total mass of Ag, at ±1 kV the mean deposited masses of AgNPs were 0.42, 1.3 and 2.1 $\mu g\ cm^{-2}$ for flow rates of 100, 214 and 390 ml min^{-1}, respectively. The corresponding mean values were 0.89, 1.5 and 2.2 $\mu g\ cm^{-2}$ when changing the field strength to ±2 kV. The deposition efficiency of Ag was verified chemically for a selection of samples using AAS (Table 1). The amount of cellular Ag, after 2 h exposure to AgNPs at ±1 kV and with flow rates of 214 and 390 ml min^{-1}, were determined chemically to mean values of 0.45 and

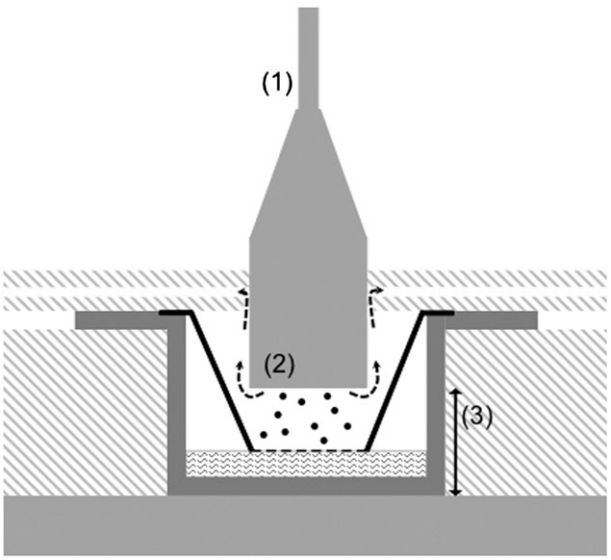

Figure 3. Cross-section of an exposure chamber showing the airflow pattern. Aerosol is led to the cells by a pump and critical orifice airflow controllers. (1) Tube diameter: 4.72 mm. (2) Diameter of the aerosol inlet: 20.4mm. Particle deposition is enhanced by an electrostatic force between two electrodes: aerosol inlet and metal plate underneath the exposure chamber. (3) Distance between the electrodes: 10.5 mm.

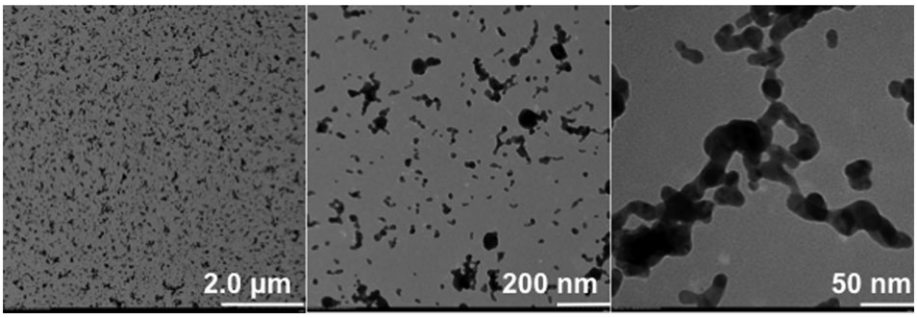

Figure 4. Transmission electron microscopy images of freshly generated silver nanoparticles deposited on the cell culture inserts with an aerosol flow rate of 214 ml min^{-1} and applied electrostatic field strength of ±1 kV. Images show a relatively uniform particle deposition pattern as well as the particle size and agglomeration state.

Table 1. Deposited amounts of Ag on transwell membranes and in the cell layer (cellular dose) measured by means of gravimetry (dry weight) and by AAS after 2 h of exposure at different aerosol flow rates (100, 214 and 390 ml min^{-1}) and applied electrostatic field strengths (±1 or ±2 kV). The figures represent the mean value of three independent experiments and standard deviations of the mean (±SD)

Flow rate (ml min^{-1})	Electrostatic field (kV)	Ag concentration (µg cm^{-2})		
		Weight	AAS	Cell dose
100	1	0.42 ± 0.12	0.52 ± 0.12	
	2	0.89 ± 0.12	0.67 ± 0.17	
214	1	1.3 ± 0.14		0.45 ± 0.23
	2	1.5 ± 0.14		
390	1	2.1 ± 0.24	1.69 ± 0.55	0.74 ± 0.29
	2	2.2 ± 0.12	1.43 ± 0.82	

AAS, atomic absorption spectroscopy.

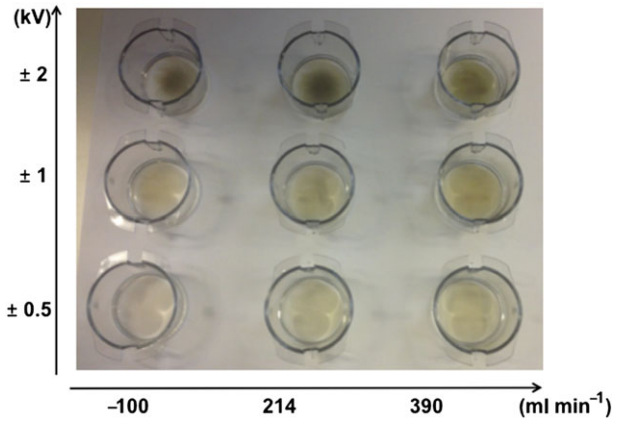

Figure 5. Examples of cell culture inserts used for visual characterization of the deposition pattern of silver nanoparticles for different aerosol flow rates (100, 214 and 390 ml min^{-1}) and applied strengths of the electrostatic field (±0.5, ±1 and ±2 kV).

0.74 µg cm^{-2}, respectively (Table 1). Thus, a stronger electrostatic field and an increased aerosol flow rate enhance the deposition efficiency of AgNPs.

The effects of aerosol flow rate (100, 214 and 390 ml min^{-1}) and applied electrostatic field strength (±0.5, ±1 and ±2 kV) on the deposition pattern of AgNPs (i.e,, how evenly particles deposit) on the surface of the insert membranes are shown in Fig. 5. Based on these visual investigations, the distribution of deposited AgNPs is relatively uniform at applied electrostatic fields of ±0.5 and ±1 kV (Fig. 5). The deposition pattern, however, is less uniform when the electrostatic field is increased to ±2 kV, i.e., the particles congregated towards the center of the membrane. This image also illustrates the enhanced particle deposition both with increased strength of the applied electrostatic field and with increased aerosol flow rate. TEM images, recorded after AgNP deposition at similar conditions as in the cell exposures (2 h, 214 ml min^{-1} and ±1 kV), also revealed a uniform particle deposition pattern (Fig. 4).

The particle size distributions that were measured from the aerosol downstream of the exposure system further describe how the electrostatic field affects the amount of deposited particles (Fig. 6). Furthermore, there is a clear shift in the particle size distribution depending on the strength of the electrostatic field (Fig. 6).

Cell viability

Cell viability in terms of cell membrane integrity and metabolic activity of A549 cells after exposure to clean air and AgNPs at different experimental conditions in the ALI system are presented in Fig. 7. Following 2 h clean air exposure, there were no significant differences in cell viability or cellular metabolic activity compared to the controls. Similarly, no effects were observed following 2 h exposure to clean air at an applied electrostatic field strength of ±1 kV. Thus, the viability of A549 cells was not affected by the ALI system set-up (Fig. 7). However, the metabolic activity was

Journal of Applied Toxicology

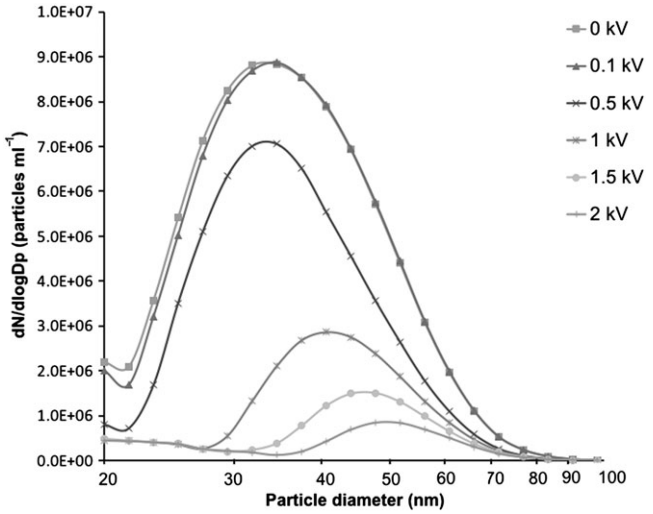

Figure 6. Particle size distributions in the aerosol containing polydisperse silver nanoparticles measured in the air exiting the air–liquid interface exposure system using a differential mobility particle sizer. Each curve represents different strengths of the applied electrostatic field: 0, ±0.1, ±0.5, ±1, ±1.5 and ±2 kV.

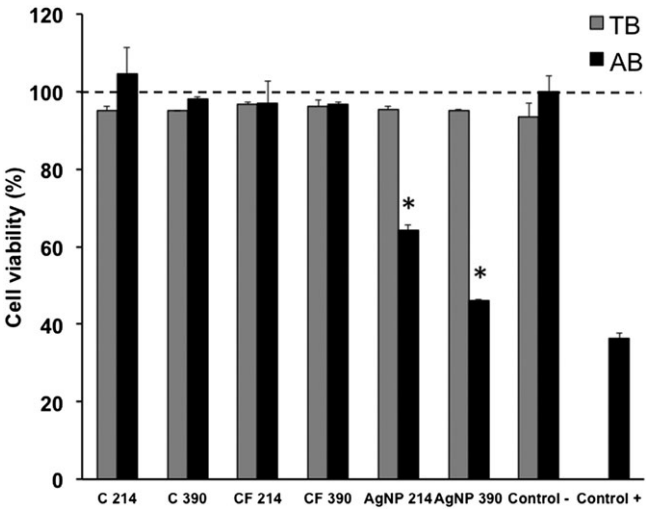

Figure 7. Viability of A549 cells analyzed with TB and AB assays after 2 h exposure in the air–liquid interface system with six different treatments (AgNP 214, AgNP 390, C 214, C 390, CF 214, CF 390). AB values are relative compared to cell viabilities in control treatments (Control–, Control+). Asterisk is assigned for statistically significant ($P < 0.05$) values. Each bar represents the mean value of three independent experiments. Error bars represent the standard deviation of the mean value (±SD). AB, alamar blue; AgNP, silver nanoparticle; AgNP 214, AgNP aerosol at 214 ml min^{-1} and ±1 kV; AgNP 390, AgNP aerosol at 390 ml min^{-1} and ±1 kV; C 214, clean air at 214 ml min^{-1}; C 390, clean air at 390 ml min^{-1}; CF 214, clean filtered air at 214 ml min^{-1} and ±1 kV; CF 390, clean filtered air at 390 ml min^{-1} and ±1 kV; Control–, incubator control cells; Control+, cells exposed to CuO nanoparticle dispersion at a concentration of 40 μg cm^{-2}; TB, trypan blue.

reduced to 64 and 46% following exposure to AgNPs at similar conditions (Fig. 7). These levels of metabolic activity were significantly lower compared to findings for the clean air exposures. Measured amounts of Ag on the cell cultures at these conditions were 0.45 and 0.74 μg cm^{-2}, respectively (Table 1). The membrane integrity of the cells was not affected.

Discussion

This study has focused on the optimization of an ALI exposure system for assessing the toxicity of airborne NPs in human lung cells. The influence of different exposure conditions on the deposition efficiency of airborne NPs on to lung cell cultures was evaluated using AgNPs as model particles.

The amount of deposited Ag in our study ranged from 0.42 to 2.2 μg cm^{-2}, depending on the aerosol flow rate (100, 214 and 390 ml min^{-1}) and the strength of the electrostatic field (±1 or ±2 kV), based on the results of both gravimetric and chemical analysis (Table 1). These amounts are roughly in the same range as in other ALI *in vitro* studies (Herzog *et al.*, 2013; Holder & Marr, 2013) and close to model estimates of relevant exposure levels in humans (Gangwal *et al.*, 2011). The model by Gangwal *et al.* is based on the highest air concentration of AgNPs (with diameters of 5–100 nm) measured at different nanomaterial manufacturing, research and development sites. By assuming a continuous exposure over the course of 24 h, the model estimates, that alveolar Ag levels in the range 0.061–0.15 μg cm^{-2} can be reached (Gangwal *et al.*, 2011). Translated into a full working life exposure (45 years, 5 days per week, 8 h per day), and taking into account particle clearance, this corresponds to total accumulation of 2.0–4.9 μg cm^{-2} Ag in the alveoli (Gangwal *et al.*, 2011). According to these exposure estimations, the deposited amounts of Ag obtained in our study represent roughly a scenario of 72–120 h of continuous exposure, or approximately 3–11 years of exposure during working hours. Thus, it was concluded, that efficient deposition of AgNPs could be achieved with the current ALI system set-up described in this study. Based on these results, the deposition efficiency of AgNPs was clearly enhanced both when applying stronger electrostatic fields and increased aerosol flow rates (Table 1, Fig. 5).

An interesting observation from the Ag deposition analyses in this study, is that the amount of Ag was in general higher (approximately 2.5–3 times) in the cell-free insert membranes compared to the amount of Ag deposited on the cells (Table 1). Despite the possible underestimations of the cellular Ag mass due to the formation of insoluble AgCl complexes and their interference during the measurements of cellular Ag, this observation suggests that cellular deposition cannot be estimated solely based on deposition analyses at cell-free conditions. Additionally, in our previous publication describing the exposure of lung cells to airborne CuNPs in ALI, we measured substantial differences in the particle deposition efficiency at cell-free conditions compared to conditions with cells (Elihn *et al.*, 2013). In the previous work, however, the measured differences in the Cu amounts may also be explained by the release of Cu ions into the cell media in the presence of cells. The release of Ag^+ ions into cell media might also be one factor behind the observed differences in cellular and cell-free conditions in our current study, although this is considered unlikely. Based on the findings in a previous study, the release of Ag from uncoated AgNPs in cell media can be estimated to be < 5% during short-term (< 24 h) exposures (Gliga *et al.*, 2014). Therefore, this would not explain the observed differences between Ag masses in this study.

The enhancement of AgNP deposition by increasing the electrostatic field strength was also clear when the particle concentrations were measured in the aerosol exiting the exposure system (Fig. 6). Even though these measured aerosol particle concentrations cannot be directly translated into quantifiable levels of particle deposition on the insert membranes, they underline the importance of the electrostatic field for the deposition of

nano-sized particles in this exposure system. For example, when estimating the particle deposition efficiency based on measured differences in particle concentrations up- and downstream of the exposure system, only 2% of the particles were deposited at an applied electrostatic field strength of ±0.1 kV. At ±0.5 kV, the deposition efficiency increases to 34% and even further at ±1 kV (79%), ±1.5 kV (89%) and ±2 kV (94%). When the particle deposition is compared to previous methods, it is further emphasized that the use of an applied electrostatic field clearly enhances the deposition of nano-sized particles (Elihn *et al.*, 2013).

Despite the enhanced deposition efficiency, there are limitations to the use of an electrostatic field. For the first, it affects how evenly the particles deposit on the insert membranes. AgNPs were distributed relatively evenly on the membranes at applied electrostatic fields of ±0.5 and ±1 kV (Fig. 5). However, at ±2 kV it was evident that the particles congregated towards the center of the membrane. This implies that to achieve the most uniform particle deposition pattern, the applied electrostatic field strength should be lower than ±2 kV. For the second, in the aerosol exiting the exposure system, the particle size distributions shifted along with the changing electrostatic field (Fig. 6). This was expected, as the deposition of larger-sized particles requires a stronger electrostatic force compared to smaller particles (Hinds, 1999). These observed changes in particle size distributions, measured downstream the exposure system, illustrate a comparable (but opposite) change in the size distribution of the deposited particles.

To study whether the exposure system or the different exposure conditions affect the viability and metabolic activity of A549 cells, the cells were first exposed to clean air. After no effects were observed following 2 h exposure to clean air at an applied electrostatic field strength of ±1 kV with an aerosol flow rate of 214 or 390 ml min^{-1}, it was concluded that the ALI exposure system, in these conditions, does not by itself induce cytotoxicity of A549 cells. Then, the performance of the exposure system was evaluated further by exposing the cells to AgNPs. Exposure of A549 cells to AgNPs at 0.45 and 0.74 μg cm^{-2} induced significant reductions in the cellular metabolic activity after 2 h. However, no effects on cell viability in terms of membrane damage were observed within the same period. Because cytotoxic responses have been reported for AgNPs previously, the reduced metabolic activity by AgNP exposure in our study was expected. The observed cytotoxicity of AgNPs in lung cells varies between different studies (Carlson *et al.*, 2008; Foldbjerg *et al.*, 2011; Gliga *et al.*, 2014). Owing to several differences in exposure set-ups between the studies, such as the presence of surface coatings on the particles and varying physicochemical properties of the particles, any direct comparisons with literature findings are not straightforward or apparent. For instance Herzog *et al.* (2013) reported no increased cytotoxicity (activity of lactate dehydrogenase) after exposing co-cultured lung cells in ALI to citrate-coated AgNPs at concentrations of 0.030 and 0.278 μg cm^{-2} for 4 and 24 h. This is in line with our study showing no effect on membrane integrity. Another study by Holder and Marr (2013) reported only minor cytotoxic and inflammatory responses in A549 cells cultured in ALI when exposed to non-coated AgNPs at a concentration of 0.7 μg cm^{-2} for 24 h. One underlying factor for the different results of AgNP toxicity might be that the bioavailability of AgNPs is strongly affected by different extracellular conditions such as pH and the presence of ions, proteins, lipids and other species forming Ag complexes. The bioavailability is also affected by the diverse intracellular conditions in different cellular compartments (Behra *et al.*, 2013).

The release of Ag^+ ions from AgNPs is possibly the most recognized property behind their toxic effects. For example, the antimicrobial effects of AgNPs are mainly attributed to the release of Ag^+ ions (Sondi & Salopek-Sondi, 2004). Whether the reduced cellular metabolism upon AgNP exposure, seen in our study, was caused by particles, by released Ag from the particles, or by their combination, is impossible to establish in this study. However, due to the relatively slow oxidation and transformation (dissolution) rate of AgNPs (Liu & Hurt, 2010) and the short time (< 10 s) for the particles to interact with moisture in the aerosol, it is likely that the major fraction of the AgNPs in the aerosol was present as particles upon cell deposition. The predominance of AgNPs as particles on the cell culture inserts was also confirmed with TEM (Fig. 4).

In relation to the mechanisms behind the AgNP-induced cytotoxicity, the observed lack of effects on cell membrane damage and the simultaneous reduction in cellular metabolic activity may advocate that AgNPs in this study act primarily through another route as opposed to direct disruption of the cell membrane. However, it is likely that membrane damage would take place upon prolonged exposure. In addition to direct effects of particles or released Ag species on the cells, reactive oxygen species (ROS), both triggered by surface reactions on the AgNPs and released from mitochondria, have been suggested to be an important aspect for the toxicity of AgNPs (Carlson *et al.*, 2008; Foldbjerg *et al.*, 2011; Joshi *et al.*, 2015). One proposed mechanism for AgNPs, possibly related to ROS, is the disruption of the mitochondrial respiratory chain (AshaRani *et al.*, 2009). AgNPs have also been shown to induce the production of ROS while reducing the mitochondrial activity in A549 cells at a corresponding cellular Ag concentration range as investigated in our study (Foldbjerg *et al.*, 2011).

In conclusion, the electrostatic ALI exposure system is suitable for toxicological and mechanistic studies of airborne metal NPs in lung cells cultured at the ALI. Hence, the system can be applied as a tool in hazard characterization of airborne NPs with regard to pulmonary exposure scenarios. To improve this ALI exposure system further, our future aim is to validate its use with a co-cultured lung cell model, as such models generally are more realistic in representing the characteristics of *in vivo* lung tissue compared to monocultures (Müller *et al.*, 2009). Further studies to investigate chronic exposure scenarios will also be needed.

Acknowledgments

Grants from the Swedish Research Council for Environment, Agricultural Sciences and Spatial Planning (FORMAS) are highly acknowledged. Prof. Odnevall Wallinder and Dr. Hedberg acknowledge in addition the Swedish Research Council (VR, project no. 2013-5621) for financial support and Dr. H.L. Karlsson acknowledge funding from the Swedish Research Council for Health, Working Life and Welfare (FORTE, project no. 2011-0832).

Conflict of interest

The authors did not report any conflict of interest.

References

AshaRani PV, Low KM, Hande MP, Valiyaveettil S. 2009. Cytotoxicity and genotoxicity of silver nanoparticles in human cells. *ACS Nano* **3**: 279–290.

Behra R, Sigg L, Clift MJD, Herzog F, Minghetti M, Johnston B, Petri-Fink A, Rothen-Rutishauser B. 2013. Bioavailability of silver nanoparticles and ions: from a chemical and biochemical perspective. *J. R. Soc. Interface* **10**: 87.

Bergamaschi E. 2009. Occupational exposure to nanomaterials: Present knowledge and future development. *Nanotoxicology* **3**: 194–201.

Carlson C, Hussain SM, Schrand AM, Braydich-Stolle LK, Hess KL, Jones RL, Schlager JJ. 2008. Unique cellular interaction of silver nanoparticles: size-dependent generation of reactive oxygen species. *J. Phys. Chem. B* **112**: 13608–13619.

Cronholm P, Midander K, Karlsson HL, Elihn K, Odnevall Wallinder I, Möller L. 2011. Effect of sonication and serum proteins on copper release from copper nanoparticles and the toxicity towards lung epithelial cells. *Nanotoxicology* **5**: 269–281.

ECHA. 2015. ECHA's Regulatory Science Strategy. ECHA-15-A-01-EN.

Elihn K, Cronholm P, Karlsson HL, Midander K, Odnevall Wallinder I, Möller L. 2013. Cellular dose of partly soluble Cu particle aerosols at the air-liquid interface using an in vitro lung cell exposure system. *J. Aerosol Med. Pulm. Drug Deliv.* **26**: 84–93.

Foldbjerg R, Dang D, Autrup H. 2011. Cytotoxicity and genotoxicity of silver nanoparticles in the human lung cancer cell line, A549. *Arch. Toxicol.* **85**: 743–750.

Gangwal S, Brown JS, Wang A, Houck KA, Dix DJ, Kavlock RJ, Hubal EAC. 2011. Informing selection of nanomaterial concentrations for ToxCast in vitro testing based on occupational exposure potential. *Environ. Health Perspect.* **119**: 1539–1546.

Gliga AR, Skoglund S, Odnevall Wallinder I, Fadeel B, Karlsson HL. 2014. Size-dependent cytotoxicity of silver nanoparticles in human lung cells: the role of cellular uptake, agglomeration and Ag release. *Part. Fibre Toxicol.* **11**: 11.

Grass RN, Limbach LK, Athanassiou EK, Stark WJ. 2010. Exposure of aerosols and nanoparticle dispersions to in vitro cell cultures: A review on the dose relevance of size, mass, surface and concentration. *J. Aerosol Sci.* **41**: 1123–1142.

Hedberg J, Baresel C, Odnevall Wallinder I. 2014. Transport and fate of silver as polymer-stabilised nanoparticles and ions in a pilot wastewater treatment plant, followed by sludge digestion and disposal of sludge/soil mixtures: A case study. *J. Environ. Sci. Health A* **49**: 1416–1424.

Herzog F, Clift MJD, Piccapietra F, Behra R, Schmid O, Petri-Fink A, Rothen-Rutishauser B. 2013. Exposure of silver-nanoparticles and silver-ions to lung cells in vitro at the air-liquid interface. *Part. Fibre Toxicol.* **10**: 11.

Hinds WC. 1999. *Aerosol Technology*: *Properties*, *Behavior*, *and Measurement of Airborne Particles*, 2nd edn. John Wiley & Sons, Inc.: Hoboken, NJ, USA.

Holder AL, Marr LC. 2013. Toxicity of silver nanoparticles at the air-liquid interface. *Biomed. Res. Int.* **2013**: 1–11.

ICRP. 1994. *Human Respiratory Tract Model for Radiological Protection* 66: 1–3.

Joshi N, Ngwenya BT, Butler IB, French CE. 2015. Use of bioreporters and deletion mutants reveals ionic silver and ROS to be equally important in silver nanotoxicity. *J. Hazard. Mater.* **287**: 51–58.

Karlsson HL, Cronholm P, Gustafsson J, Möller L. 2008. Copper oxide nanoparticles are highly toxic: a comparison between metal oxide nanoparticles and carbon nanotubes. *Chem. Res. Toxicol.* **21**: 1726–1732.

Karlsson HL, Gustafsson J, Cronholm P, Möller L. 2009. Size-dependent toxicity of metal oxide particles – a comparison between nano- and micrometer size. *Toxicol. Lett.* **188**: 112–118.

Karlsson HL, Cronholm P, Hedberg Y, Tornberg M, De Battice L, Svedhem S, Odnevall Wallinder I. 2013. Cell membrane damage and protein interaction induced by copper containing nanoparticles – Importance of the metal release process. *Toxicology* **313**: 59–69.

Kim JS, Peters TM, O'Shaughnessy PT, Adamcakova-Dodd A, Thorne PS. 2013. Validation of an in vitro exposure system for toxicity assessment of air-delivered nanomaterials. *Toxicol. In Vitro* **27**: 164–173.

Lenz AG, Karg E, Lentner B, Dittrich V, Brandenberger C, Rothen-Rutishauser B, Schulz H, Ferron GA, Schmid O. 2009. A dose-controlled system for air-liquid interface cell exposure and application to zinc oxide nanoparticles. *Part. Fibre Toxicol.* **6**: 32.

Limbach LK, Li Y, Grass RN, Brunner TJ, Hintermann MA, Muller M, Gunther D, Stark WJ. 2005. Oxide nanoparticle uptake in human lung fibroblasts: effects of particle size, agglomeration, and diffusion at low concentrations. *Environ. Sci. Technol.* **39**: 9370–9376.

Liu J, Hurt RH. 2010. Ion release kinetics and particle persistence in aqueous nano-silver colloids. *Environ. Sci. Technol.* **44**: 2169–2175.

Lundqvist M, Stigler J, Elia G, Lynch I, Cedervall T, Dawson KA. 2008. Nanoparticle size and surface properties determine the protein corona with possible implications for biological impacts. *Proc. Natl. Acad. Sci. U. S. A.* **105**: 14265–14270.

Müller L, Riediker M, Wick P, Mohr M, Gehr P, Rothen-Rutishauser B. 2009. Oxidative stress and inflammation response after nanoparticle exposure: differences between human lung cell monocultures and an advanced three-dimensional model of the human epithelial airways. *J. R. Soc. Interface* **7**: S27–S40.

Oberdörster G, Oberdörster E, Oberdörster J. 2005. Nanotoxicology: an emerging discipline evolving from studies of ultrafine particles. *Environ. Health Perspect.* **113**: 823–839.

Paur H, Cassee FR, Teeguarden J, Fissan H, Diabate S, Aufderheide M, Kreyling WG, Hänninen O, Kasper G, Riediker M, Rothen-Rutishauser B, Schmid O. 2011. In-vitro cell exposure studies for the assessment of nanoparticle toxicity in the lung – A dialog between aerosol science and biology. *J. Aerosol Sci.* **42**: 668–692.

Russell WMS, Burch RL, Hume CW. 1959. *The Principles of Humane Experimental Technique*. http://altweb.jhsph.edu/pubs/books/humane_exp/addendum (accessed 13 November 2015).

Savi M, Kalberer M, Lang D, Ryser M, Fierz M, Gaschen A, Rička J, Geiser M. 2008. A novel exposure system for the efficient and controlled deposition of aerosol particles onto cell cultures. *Environ. Sci. Technol.* **42**: 5667–5674.

Schäfer B, Brocke J, Epp A, Götz M, Herzberg F, Kneuer C, Sommer Y, Tentschert J, Noll M, Günther I, Banasiak U, Böl G, Lampen A, Luch A, Hensel A. 2013. State of the art in human risk assessment of silver compounds in consumer products: a conference report on silver and nanosilver held at the BfR in 2012. *Arch. Toxicol.* **87**: 2249–2262.

Sondi I, Salopek-Sondi B. 2004. Silver nanoparticles as antimicrobial agent: a case study on *E. coli* as a model for Gram-negative bacteria. *J. Colloid Interface Sci.* **275**: 177–182.

Tarimala S, Kothari N, Abidi N, Hequet E, Fralick J, Dai LL. 2006. New approach to antibacterial treatment of cotton fabric with silver nanoparticle-doped silica using sol-gel process. *J. Appl. Polym. Sci.* **101**: 2938–2943.

Teeguarden JG, Hinderliter PM, Orr G, Thrall BD, Pounds JG. 2007. Particokinetics in vitro: Dosimetry considerations for in vitro nanoparticle toxicity assessments. *Toxicol. Sci.* **95**: 300–312.

Wittmaack K 2011a. Excessive delivery of nanostructured matter to submersed cells caused by rapid gravitational settling. *ACS Nano* **5**: 3766–3778.

Wittmaack K 2011b. Novel dose metric for apparent cytotoxicity effects generated by in vitro cell exposure to silica nanoparticles. *Chem. Res. Toxicol.* **24**: 150–158.